Diffuse-x-ray-scattering measurements of roughness on ion-etched multilayer interfaces

R. Schlatmann, J. D. Shindler, and J. Verhoeven
FOM Institute for Atomic and Molecular Physics, Kruislaan 407, 1098 SJ Amsterdam, The Netherlands
(Received 25 July 1994)

The effect of ion etching on the interface morphologies of Mo/Si multilayers is investigated via measurements of small-angle diffuse scattering. A comparison is made between two electron-beam-deposited multilayers composed of ten Mo/Si double layers, one with each surface ion etched after deposition. It is observed that ion etching preferentially reduces the short-length-scale interfacial roughness. The non-ion-etched sample exhibits a nearly constant diffusely scattered intensity as a function of in-plane momentum transfer (q_x) over the measurable q_x range. Thus, roughness contributions from very small length scales are dominant. In contrast, the ion-etched sample produces an exponential decay in the diffuse intensity as a function of q_x, which is quantitatively inconsistent with predicted line shapes of existing models describing the effect of ion etching on surface morphology. The data is fit by a model that includes an algebraic decay of the real-space height-height correlations. Possible causes for the discrepancy between data and theory are discussed.

I. INTRODUCTION

Multilayers are one-dimensional synthetic structures, consisting of a number of alternating layers. They find a wide range of (x-ray) optical, mechanical, magnetic, or electrical applications. In most of the applications, the quality of the multilayer is determined by the nature of the interfaces. More specifically, the width of the interface, resulting from interdiffusion or from roughness, and the in-plane sizes of the deviations from the average interface are the main characteristics of a nonideal interface.

The multilayers that we have studied were specifically designed for the reflection of soft x rays.[1] The reflection of x rays by multilayers is based on the constructive interference of the x rays (weakly) reflected by each of the interfaces. The Bragg formula gives the condition for constructive interference for a given multilayer period, wavelength, and angle. For this application it means that the period of the multilayers is of the order of the soft-x-ray wavelength, being several nm.

In previous experiments[2–5] it has been shown that rough surfaces can be smoothed significantly by ion etching. The essential step of this process, when making multilayers, is that an excess layer of material is removed by ion sputtering, during which surface roughness can be reduced. This results in higher x-ray reflectivities. Since we have separate steps of growth and ion etching, we can disentangle the effects on surface morphology of growth and low-energy ion impact, which occur simultaneously in the widely used techniques of ion beam assisted deposition and sputter deposition. Besides, low-energy ion impact is also one of the processes that occur during reactive ion etching and surface cleaning. As the exact mechanism of the ion etching process is still unresolved, this paper is mainly concerned with the in plane length scales of the roughness of multilayer interfaces grown with and without ion etching. These we will describe, as is usually done, in terms of a two point height-height correlation function. This function can be defined in real space as a function of in-plane lengths or in reciprocal space as a function of in-plane spatial frequencies, and the two are connected by a straight Fourier transform.

There has been extensive theoretical research on the development of microscopic surface morphology during growth of thin films (see, for instance, Refs. 6–8) and multilayers[9,10] and a significantly smaller number of papers on the effects of ion-beam erosion.[8,11] From the numerous measurements of surface morphologies, using a host of techniques such as x-ray and electron reflectivity, scanning probe microscopy (STM and AFM), ellipsometry, and electron microscopy, the papers most closely related to our present study include a number of x-ray reflectivity studies on multilayers[10,12,13] and ion etched SiO_2 surfaces,[5] as well as an STM study of ion-etched graphite.[14]

X-ray reflectivity is one of the techniques that can probe the length scales of interest in the problem of surface roughness. In many areas of materials research, on both solids[15,16] and liquids,[17–19] diffuse x-ray scattering has also been used to gain insight into the lateral distribution of surface undulations. The technique has the advantage that it is nondestructive, that it can probe relatively large sample areas (of the order of a few mm^2), and that all interfaces can be probed simultaneously. The latter property of x-ray scattering makes it sensitive to correlations between roughness at different interfaces, but it also complicates the extraction of detailed information on specific interfaces of a multilayer. Furthermore, the information obtained is in reciprocal space, not real space.

In this paper, we report on diffuse x-ray-scattering measurements made on Mo/Si multilayers, prepared with and without ion etching. We will first describe sample preparation and the optimization of the reflectivity setup to measure the properties of interest. After defining the

0163-1829/95/51(8)/5345(7)/$06.00 ©1995 The American Physical Society

method of analysis, the incompatibility of our data with existing models will be demonstrated. We will suggest an alternative height-height correlation function, which allows us to fit the data. We will also show how we can use the data to split the total interfacial width into a scattering (rough) and nonscattering (intermixed) part. In the discussion, various causes for the discrepancy between data and theory are considered.

II. EXPERIMENT

A. Sample deposition

The multilayers were deposited on 10×25-mm^2 substrates, cut from Si (111) wafers from which we did not remove the native oxide layers. We used an UHV (base pressure 10^{-7} Pa) electron-beam evaporation system.[20] All layers were deposited at a rate of 0.01 nm/s. Since we did not heat or cool the substrates during deposition the estimated substrate temperature during Mo deposition (350 K) was slightly higher than during Si deposition (300 K). For ion-beam etching, we used a Kaufman source with a 3-cm beam diameter. The 300-eV Kr^+ ions were incident at an angle of 45° with the surface normal, with a flux of 10^{14} ions/cm^2 sec. The excess layer thickness removed from each of the layers after deposition was 1.3 nm, corresponding to a fluence of 1.2×10^{16} ions/cm^2. The layer thicknesses during deposition and ion etching were controlled by *in situ* soft-x-ray reflectivity. For these multilayers the soft-x-ray line used was C-$K\alpha$, with a wavelength $\lambda=4.47$ nm. Given the grazing angle of incidence of 25° and the optical constants of the materials deposited, the Bragg relation gives an interference period in the measured reflectivity signal of about 6 nm. Each of the multilayers used in the x-ray-scattering experiments consisted of 10 periods of Mo and Si layers, covered with a 6-nm Si layer to exclude atmospheric influences on the actual multilayer itself.

B. X-ray-scattering setup

The x-ray generator is an Enraf-Nonius GX-21, operated at 8 kW maximum power. In the scattering configuration described below, we obtain a main beam of 8.4×10^8 photons/sec incident on the sample. The sample was enclosed in an evacuated cell to reduce nonsample background scattering to near dark-count levels of ≈0.05 counts/sec. This allowed a dynamic range of nearly ten orders of magnitude in the measured intensity, enabling us to probe very small in-plane length scales.

Details of the scattering configuration are described elsewhere.[21] In brief, it employs a bent graphite monochromator which focuses the beam in the out-of-plane direction onto the sample. Although both Cu-$K\alpha_1$ and Cu-$K\alpha_2$ lines are selected with this monochromator, the moderate resolution obtained is dominated by the angular beam divergence. The incident in-plane beam divergence, $\Delta\alpha$, is defined by a slit set between the monochromator and the sample, while slits immediately before a scintillation detector define the in-plane detector acceptance, $\Delta\beta$. Out of the scattering plane, all slits are left wide open. Thus, we effectively integrate the intensity in this direction. For this work, $\Delta\alpha=\Delta\beta=0.08°$ full width at half maximum. Such symmetric resolution is advantageous for diffuse scattering measurements, as opposed to the usual case where the emphasis is on the measurement of the specular signal and typically $\Delta\alpha\ll\Delta\beta$. In this paper, fitted models include a convolution with resolution.

The beam size at the sample was approximately 0.2×3 mm^2, while the samples themselves were 25×10 mm^2. Thus, overfilling of the sample occurred for incident angles $\alpha\leq0.5°$. In addition, when the detector angle $\beta\gg\alpha$ and α small, the signal may also be reduced if the beam footprint on the sample is larger than the sample area visible by the detector. This latter effect is one possible cause of asymmetry in transverse sample rocking scans. Both of these geometrical effects have been corrected for in the data shown.

III. RESULTS

In the experiments described, we have taken three types of scans: Specular reflectivity scans, in which the grazing angle of incidence α of the x rays is equal to the outgoing angle β, off-specular scans where the sample is offset from the specular condition by a small angle ω, such that $\omega=(\beta-\alpha)/2$, and the transverse scans, where ω is varied, but the total scattering angle $\alpha+\beta$ is kept

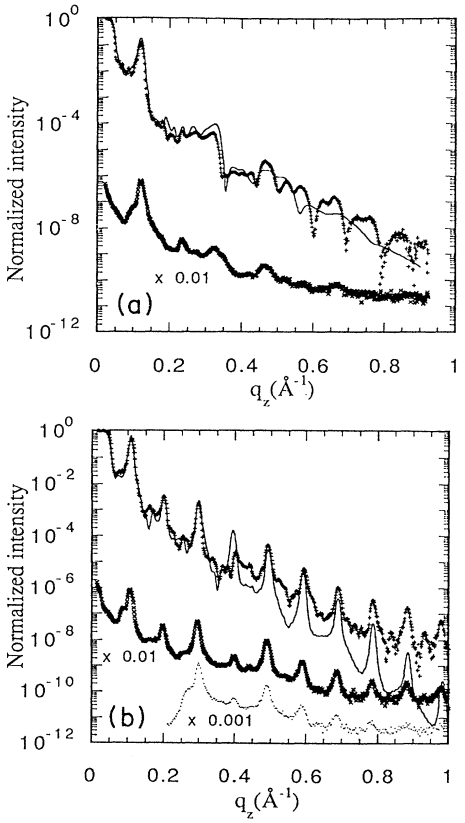

FIG. 1. (a) Specular intensity (+) and off-specular (×) intensity at offset angle $\omega=0.15°$ from as-deposited sample. (b) Specular intensity (+) and off-specular intensity [at $\omega=0.15°$ (×) and $\omega=1.5°$ (●)] from an ion-etched sample. Symbols represent measured intensities, solid lines represent fits. For clarity off-specular scans have been shifted.

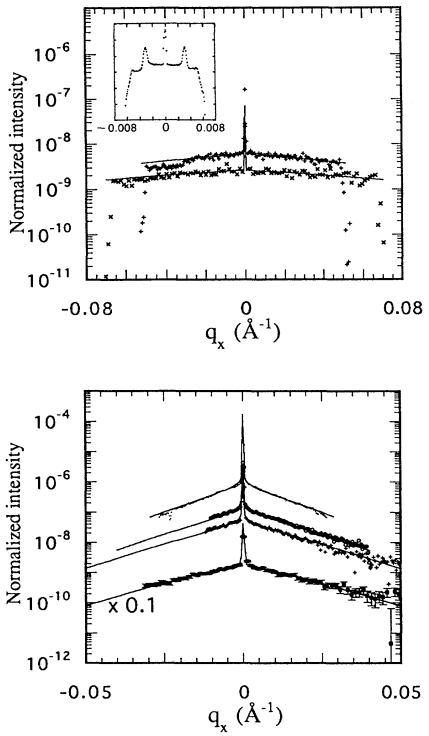

FIG. 2. (a) Transverse scan intensities from as-deposited sample at $q_z=0.66$ Å^{-1} (+) and $q_z=0.76$ Å^{-1} (×). The sharp drop in intensity at the critical angle shows that the data is far above background. The inset shows strong dynamical peaks in a transverse scan at $q_z=0.23$ Å^{-1}. (b) Transverse scan intensities from an ion-etched sample at $q_z=0.49$ (●), 0.59 (○), 0.69 (+), and 0.79 (□) Å^{-1}. For clarity the lowest curve has been shifted and points beyond the critical angle have been removed. Symbols represent measured intensities, solid lines represent fits using the model explained in the text.

fixed. If the wave vector $\mathbf{k}$, with $|\mathbf{k}|=2\pi/\lambda$, and the wave-vector transfer $\mathbf{q}=\mathbf{k}_{\text{out}}-\mathbf{k}_{\text{in}}$ are defined, one can derive the reciprocal space equivalent of these scans. The spatial coordinates are chosen such that the surface normal is along $\hat{z}$, and, thus, specular scans probe only in the q_z direction, i.e., perpendicular to the interfaces. From these scans, we extract the spacing of the interfaces and the total interfacial widths. Off-specular scans probe in both q_z and q_x (in-plane) directions, and are used to measure the degree of conformality of roughness at different interfaces. Transverse scans mainly probe along the q_x, i.e., in-plane direction (for $\alpha+\beta$ small) and, therefore, yield the information of most interest to this experiment. In the next section, we will show how transverse scans are connected to the interfacial correlation function that we are interested in.

All x-ray-scattering measurements shown have been normalized to the incident-beam intensity. The true specular signal has been obtained by subtracting the off-specular scan (offset angle $\omega=0.15°$) from the raw specular signal. In this way, the diffuse contribution at $q_x=0$ is almost completely removed. Figure 1 shows specular and off-specular scans for both samples.

All transverse scans shown have been footprint and background corrected, and have also been corrected for the changing coherence length of the beam on the sample during the scan ($1/\sin\alpha$ correction). Background levels were calculated from points at which $\alpha\leq 0$ or $\beta\leq 0$. Data around several orders of Bragg peaks are shown in Fig. 2.

IV. THEORY

To analyze our data, we split the calculated intensity into a specular and a diffuse part. To fit the specular signal, we use the recursive dynamical method of Parratt.[22] To analyze the diffuse part of the x-ray scattering, we make use of the formalism developed by Sinha *et al.*[15] They have shown that in the first Born approximation for a single surface the scattering cross section per unit area surface is given by

$$S(\mathbf{q})=(r_e\Delta\rho)^2\frac{e^{-q_z^2\sigma_t^2}}{q_z^2}\int\int_{S_0}dx\,dy\,e^{q_z^2C(x,y)}\times e^{-i(q_xx+q_yy)}, \quad (1)$$

where the integral is over the coherence area of the beam on the sample. The term $\Delta\rho$ gives the change in electron density at the interface, and r_e is the classical electron radius. With $u(x,y)$ the height of the interface at an arbitrary in-plane position (x,y), a height-height correlation function has been defined as $C(x,y)=\langle u(x,y)u(0,0)\rangle$, the brackets denoting a statistical average over the whole surface, where $C(0,0)=\sigma_r^2$. The total interfacial width is given by this roughness contribution σ_r and by an intermixing contribution σ_m. Because both contributions are assumed to be independent Gaussian random variables, the total width σ_t is found by addition in quadrature of the contributing widths, i.e., $\sigma_t^2=\sigma_r^2+\sigma_m^2$.[23] The intermixing can be assumed to be uncorrelated, or zero length scale roughness. It will not cause diffuse scattering, but it will lower the specular intensity which is sensitive to the total interfacial width.

Corrected for geometrical factors as beam width, sample area and slit sizes, and convolved with the resolution function at fixed q_z, $S(\mathbf{q})$ is proportional to the measured intensity as a function of q_x.

One can extend the derivation to the case of scattering from multilayers and account for refraction and absorption by calculating the complex scattering vectors inside the multilayers. Then, if one also explicitly integrates over one in-plane direction in $\mathbf{q}$, let us say q_y, to account for the fact that the detector slit is wide open in that direction,[15] one can find for the diffuse part of $S(\mathbf{q})$:

$$S_{\text{diff}}(q_x)=\int_{-\infty}^{\infty}S_{\text{diff}}(\mathbf{q})dq_y = \sum_{i=1}^{N}\sum_{j=1}^{N}r_e^2\Delta\rho_i\Delta\rho_j\frac{e^{-iq_zd_{ij}}e^{-q_z^2(\sigma_{t,i}^2+\sigma_{t,j}^2)/2}}{q_z^2}\times\int_{-\infty}^{\infty}dx\,(e^{q_z^2C_{i,j}(x)}-1)e^{-iq_xx}, \quad (2)$$

where the double sum runs over all N interfaces, each

with a certain width σ_t. The term d_{ij} denotes the distance between the average position of the interfaces i and j. Note that the specular part of the scattering has been explicitly subtracted out. The correlation function $C(x)$, assuming isotropic interfaces, now has been defined to include correlations in as well as across interfaces: $C_{i,j}(x)=\langle u_i(x)u_j(0)\rangle$. If such cross-correlations exist, i.e., if $C_{i,j}(x)$ is nonzero for some $i\neq j$, then the exponential term with $q_z d_{ij}$ as the phase gives the interference between diffusely scattered amplitudes. Such interference gives rise to Bragg peaks in the diffuse intensity,[12] measured as a function of q_z.

It can be seen that $S_{\text{diff}}(q_x)$ for $q_z\sigma_r \ll 1$ is directly proportional to the Fourier transform of the interfacial correlation function.[15] However, at Bragg angles close to the critical angle for total reflection, these multilayers are very strong scatterers. This means that for tne analysis of transverse scans at low q_z, such as shown in the inset of Fig. 2(a), a dynamical theory is needed. This type of theory was also developed by Sinha *et al.* for a single interface and extended to the case of multilayers in a recent paper by Holy *et al.*[24] It essentially involves a dynamical calculation of the total electric field at each of the interfaces, with those values as prefactors to the integral in Eq. (2). When the incident or exit angles equal a lower order Bragg angle, the electric fields of incoming and outgoing waves have similar amplitudes and add in phase, and the total electric field, and, thus, the diffuse intensity, is enhanced. For multilayers one can then observe so-called "quasi-Bragg" peaks[12,25] in the diffusely scattered intensity, as a function of q_x. It may be important to note that these peaks, which are a result of the enhanced electric field in the multilayer, are not the same as the peaks that result from the correlations in roughness between different interfaces, mentioned in the previous paragraph.

However, as the measurement in the inset in Fig. 2(a) shows, the quasi-Bragg peaks can become more than a factor of 10 stronger than the diffuse scattering intensity at values of q_x around them, and existing theory underestimates the scattered intensity. Still, in transverse scans at large q_z the dynamical peaks are weak, and we can analyze these scans using Eq. (2).

V. ANALYSIS

A. As-deposited sample

The specular measurements in Fig. 1 show interference features which broaden with increasing q_z. This is an indication of a decreasing number of interfaces that can effectively contribute to the interference, which in turn is caused by an increasing interfacial roughness from substrate to surface. In a recent paper,[26] we give a detailed study and discussion of the development of σ_t as a function of layer thickness. There we found that our best fit to the specular measurement was achieved using an interfacial width ranging from 4 Å at the substrate up to 9 Å at the top surface.

In the off-specular measurement, at $\omega=0.15°$, we can see a weak reproduction of all peaks in the specular scan. This indicates some degree of conformality, as we saw in Sec. IV. Furthermore, the transverse scans taken at peaks up to $q_z=0.76$ Å^{-1} are virtually constant, whereas a loss of conformality at shorter length scales would show up as a decaying intensity at larger q_x values in these scans. From this, we conclude that conformality, i.e., the off-diagonal correlation function, must be constant down to at least the in-plane lengths probed in those scans (60 Å).

The transverse scans at high q_z values all show an almost constant intensity vs q_x [Fig. 2(a)]. Apart from the conformality mentioned in the previous paragraph, we also conclude from this that the diffuse scattering from single interfacial, i.e., on-diagonal correlation functions must be constant in q_x. This means that any model for the interfacial correlation function that can give a cutoff in reciprocal space, as formulated in a general scaling theory of Kardar *et al.*[7] will do, as long as that cutoff lies beyond our measured q_x range. In real space, this means that height-height correlations vanish very rapidly, that is, within a maximum cutoff length of 60 Å.

Physically, the result may be understood in terms of very low surface mobility of the atoms for this deposition rate and temperature. This leads to a minimal smoothing of the roughness introduced by the white noise in the deposition rate. In fact, it is the noise term that makes the interfacial width grow proportional to the square root of the multilayer thicknesses,[10,26] in the absence of relaxing mechanisms.

B. Ion-etched sample

The specular measurement from the ion-etched sample indicates that its interfacial width is smaller than that of the as deposited sample. In an earlier paper,[26] we found the fit parameters $\sigma_t=4$ and 5.5 Å for the Si-on-Mo and Mo-on-Si interfaces, respectively. This asymmetry in interfacial width was found by many authors using several deposition techniques[27,28] and also in molecular-dynamics simulations.[29] It is attributed to a difference in intermixing for the two interfaces.

The off-specular scans (Fig. 1), taken at offset angles of 0.15° and 1.5°, for this sample show a clear reproduction of all the interference structures that are visible in the specular scan, without measurable broadening. This means[12,30] that conformality of the roughness between all interfaces is nearly complete, down to in-plane length scales of less than 200 Å. Because both samples have a constant off-diagonal correlation function, we will use a single correlation function $\mathcal{C}(x)$, with $C_{i,j}(x)=\gamma\sigma_{r,i}\sigma_{r,j}\mathcal{C}(x)$ for each sample to describe each of the multilayer interfaces. By definition $\mathcal{C}(0)$ is normalized to unity. The constant γ is simply a scaling factor giving the strength of the conformality, and, therefore, of the diffuse scattering level. It does not, however, affect the shape of the correlation function, which is what we are interested in.

The transverse scans at high q_z from this sample, Fig. 2(b), show a clear difference in line shape with the scans taken from the as-deposited samples. Qualitatively, one can see that the shorter length scale (large q_x) roughness

is removed more strongly than the long length scale roughness. Remarkably, there is no observable cutoff to the roughness correlations, which means that if such a cutoff exists, it must be larger than 6000 Å.

A striking feature of all transverse scans from this sample is the exponential decay with q_x of the intensity, which is proportional to $S_{\rm diff}(q_x)$ in Eq. (2). To the best of our knowledge this is the first report of such a line shape, which can be seen to extend over a very large range of q_x values. Such a shape is inconsistent with existing models describing ion-etched surfaces.[8,11] These predict a power-law decay as a function of q_x, beyond a certain cutoff value. With these models clearly one can never fit the unambiguous data set presented here.

It should be noted that the diffuse intensity measured from this multilayer is different from that of the bare substrate [oxide covered Si (111)]. It has been shown that the diffusely scattered intensity measured from Si wafers is fitted very well by a power-law function.[19] Another point to be made is that in transverse scans at large q_z, there is a small deviation from the pure exponential form, for large q_x. We attribute this to a constant, multilayer induced background signal of 10^{-9}. We assume that it is caused by amorphous "bulk" scattering[31,32] from the layers, as opposed to interface scattering, which above this 10^{-9} background is the dominant effect. In the scans shown this background has been subtracted.

Even though existing models do not predict the line shape correctly, it is relatively easy to find a correlation function that gives a simple exponential decay of $S_{\rm diff}(q_x)$ as a function of q_x. Given Eq. (2) and the fact that the Fourier transform of a Lorentzian yields an exponential function, our simplest choice is the following correlation function:

$$C(x)=\frac{1}{1+(x/\xi)^2} . \tag{3}$$

Without claiming that this is the only function that could reproduce the data, we see that this type of correlation function corresponds to the qualitative interpretation given above. Since the r.m.s. roughness σ_r is reduced by the ion etching, the characteristic length ξ determines the shorter length scale at which roughness is reduced more strongly.

Although we cannot calculate the Fourier integral in Eq. (2) analytically with the correlation function of Eq. (3), we can make a finite order expansion of the exponential in the integral, and then integrate each term analytically. If we set $\sigma_{r,i}=\sigma_r$ for all i, which is reasonable for the ion-etched sample, we can expand in $(q_z\sigma_r)^2$, and obtain

$$S_{\rm diff}(q_x)=\sum_{i=1}^{N}\sum_{j=1}^{N} r_e^2\Delta\rho_i\Delta\rho_j \times\frac{e^{-iq_z d_{ij}}e^{-q_x^2(\sigma_{t,i}^2+\sigma_{t,j}^2)/2}}{q_z^2}\mathcal{F}(q_x) , \tag{4}$$

with

$$\mathcal{F}(q_x)=\pi\xi q_z^2\sigma_r^2 e^{-\xi q_x}\sum_{k=0}^{n}\frac{(q_z^2\sigma_r^2)^k}{k!}\sum_{l=0}^{k}a_{kl}(\xi q_x)^l , \tag{5}$$

where $a_{00}=1$, $a_{10}=\frac{1}{4}$, $a_{11}=\frac{1}{4}$, etc. For $q_z\sigma_r\ll 1$, we need only the $n=0$ term, and find an exponential line shape of $S_{\rm diff}(q_x)$, with a characteristic length that is a constant, independent of q_z. However, when $q_z\sigma_r$ increases towards unity, as is the case for much of our data, this first-order approximation breaks down. In Fig. 3, we plot the measured values of the characteristic length ξ as a function of q_z. If we also include the next order in $(q_z\sigma_r)^2$, then $S_{\rm diff}(q_x)$ can be approximated by

$$S_{\rm diff}(q_x)\propto e^{-\xi_{\rm eff}q_x} , \tag{6}$$

where

$$\xi_{\rm eff}=\xi_0[1-\tfrac{1}{4}(q_z\sigma_r)^2] . \tag{7}$$

A fit through the measured exponents then yields a value for ξ_0 and σ_r. For this multilayer, we find $\xi_0=107$ Å and $\sigma_r=1.7$ Å. Because we can determine σ_t from the specular measurement, and σ_r through the decay of the exponent $\xi_{\rm eff}$ as a function of q_z, we can now separate the contributions σ_r and σ_m, using $\sigma_t^2=\sigma_r^2+\sigma_m^2$. We find that the intermixing width ($\sigma_{m,\text{Si-on-Mo}}=3.6$ Å, $\sigma_{m,\text{Mo-on-Si}}=5.2$ Å) is larger than the roughness width ($\sigma_r=1.7$ Å). We remark that this extraction of physical information from the q_z dependence of $S_{\rm diff}(\mathbf{q})$ in transverse scans is completely analogous to the case of scattering from capillary waves on simple liquid surfaces.[18] There $S_{\rm diff}(q_x)$ decays as a power law, with an effective power $2-\eta$ where η depends on q_z^2 as well as on the surface tension.

If we calculate $S_{\rm diff}(q_x)$ numerically, we can check the validity of the values of σ_r and ξ that we found from the analytical approximation. As the fits in Fig. 2(b) show, we do indeed find a good fit to the line shapes of the scans. To compare the characteristic length of the ion-etched sample to the non-ion-etched sample, we again use the Lorentzian correlation function of Eq. (3), even though existing growth models could also fit that data well. As shown in Fig. 2(a), we find a good fit using a characteristic length ξ of the order of 20 Å. Thus, the ion etching increases the characteristic length of the

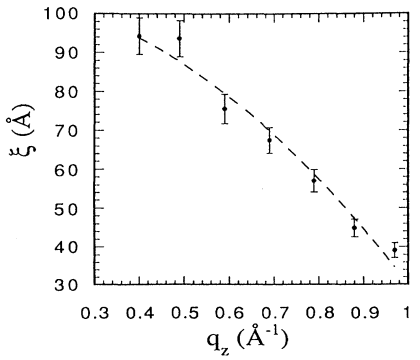

FIG. 3. Measured values in transverse scans of the effective characteristic length (see text) as a function of q_z, for an ion-etched sample. Symbols (●) represent the measured values, dashed line represents fit using the analytical approximation given in the text [Eq. (7)] for $\xi_0=107$ Å, and $\sigma_r=1.7$ Å.

roughness from 20 to 107 Å, while reducing its amplitude.

VI. DISCUSSION

It is of interest to see why the result of this measurement differs from the models mentioned. The main question that arises when we compare the ion-etched and non-ion-etched samples is do we create a new surface structure by ion etching, or does the ion-etching induced smoothing reveal a structure that already existed, but was obscured by the large amplitude, short length scale roughness? In the latter case, the measured intensity could reflect, for instance, the island size distribution of the first layer (Mo initially grows in islands[4,26]), although then one would expect to see a typical average island size, and, thus, a peak in a transverse scan. Irrespective of the cause, if what we measure is growth related rather than ion-etching related, we still could not fit the measured line shapes with existing growth models for these layer thicknesses, predicting a power-law form for $S_{\text{diff}}(q_x)$.[7]

If the measured structure is a result of the ion etching, then the assumptions which are made in the construction of the models must be checked for applicability to our samples. The assumption that the slopes on interfaces are so small that shadowing can be neglected, seems valid for these samples too. The geometry of the deposition setup is such that all atoms arrive along the surface normal. The angle of the ion beam with respect to the surface is 45° which means that shadowing could only play a role for height fluctuations at in plane length scales of the order of the r.m.s. roughness σ (≤ 10 Å). This is much smaller than our lower detection limit (≈ 60 Å).

Another implicit assumption in these models is that erosion can be treated as growth at a negative rate, ignoring specific properties of the ion-solid interaction. Although mathematically attractive, this is not necessarily true, especially for amorphous or polycrystalline films. For one, the sputtered atoms do not leave all surface positions with equal probability. Roughly speaking, atoms at peaks are more loosely bound (have a lower coordination number) than those in troughs and will, therefore, more easily be emitted from the surface. This will always have a smoothing effect, similar to the effect of shadowing.[8] Another manifestation of the unequal emission probability for different surface atoms can be found in the different sputter rates of different crystal phases,[33] which can lead to so-called preferential sputtering of certain sample areas.

Furthermore, the removal of atoms by sputtering is not a simple knock-off event, but rather one of the results of the transferal of the ion energy to the film. Other nonlocal effects can include structural relaxation[34] and crystallization[35] of the film.

Still, we should emphasize the fact that we report no more than measurements that cannot be explained by existing theory, but that we can reproduce using a mathematically simple correlation function. This correlation function, however, has no underlying physical foundation.

VII. CONCLUSION

In conclusion, we have measured the diffuse x-ray-scattering intensity from two Mo/Si multilayers, one of which had its interfaces ion etched, the other had not. We have found that the main qualitative difference in interface morphology between ion-etched and as-grown surfaces is a reduced r.m.s. roughness σ and increased characteristic length ξ. We have found that the data can be fitted using a Lorentzian real-space correlation function with a characteristic length scale of 107 Å. Using these measurements, we have decomposed the interfacial width in roughness and intermixing contributions, the latter being the dominant factor in the ion-etched sample. The measurements from the ion-etched sample are in disagreement with existing ion-etching models. We have identified possible causes for the discrepancy between our data and theory. To get an indication of how etching parameters could be incorporated in a model, we plan to do measurements in which ion energy, flux, and fluence are systematically varied.

ACKNOWLEDGMENTS

This work is part of the research program of the Stichting voor Fundamenteel Onderzoek der Materie (FOM) and was made possible by financial support from the Nederlandse Organisatie voor Wetenschappelijk Onderzoek (NWO) and the Stichting Technische Wetenschappen (STW).

[1] J. H. Underwood and T. W. Barbee, Jr., Appl. Opt. **20**, 3027 (1981).
[2] E. Spiller, Appl. Phys. Lett. **54**, 2293 (1989).
[3] E. J. Puik, M. J. van der Wiel, H. Zeijlemaker, and J. Verhoeven, Appl. Surf. Sci. **47**, 63 (1991).
[4] J. Verhoeven, C. Lu, E. J. Puik, M. J. van der Wiel, and T. P. Huijgen, Appl. Surf. Sci. **55**, 97 (1992).
[5] E. Chason and T. M. Mayer, Appl. Phys. Lett. **62**, 363 (1993).
[6] S. F. Edwards and D. R. Wilkinson, Proc. R. Soc. London Ser. A **381**, 17 (1982).
[7] M. Kardar, G. Parisi, and Y. C. Zhang, Phys. Rev. Lett. **56**, 889 (1986).
[8] G. S. Bales, R. Bruinsma, E. A. Eklund, R. P. U. Karunasiri, J. Rudnick, and A. Zangwill, Science **249**, 264 (1990).
[9] D. G. Stearns, J. Appl. Phys. **71**, 4286 (1992).
[10] E. Spiller, D. G. Stearns, and M. Krumrey, J. Appl. Phys. **74**, 107 (1993).
[11] D. G. Stearns, Appl. Phys. Lett. **62**, 1745 (1993).
[12] D. E. Savage, J. Kleiner, N. Schimke, Y. H. Phang, T. Janowski, J. Jacobs, R. Kariotis, and M. G. Lagally, J. Appl. Phys. **69**, 1 (1991).
[13] M. K. Sanyal, S. K. Sinha, and A. Gibaud, in *Interface Dy-*

namics and Growth, edited by K. S. Liang, M. P. Anderson, R. F. Bruinsma, and G. Scoles, MRS Symposia Proceedings No. 237 (Materials Research Society, Pittsburgh, 1992).
[14]E. A. Eklund, R. Bruinsma, J. Rudnick, and R. S. Williams, Phys. Rev. Lett. **67**, 1759 (1991).
[15]S. K. Sinha, E. B. Sirota, S. Garoff, and H. B. Stanley, Phys. Rev. B **38**, 2297 (1988).
[16]For an overview of surface x-ray and neutron scattering work, see *Surface X-ray and Neutron Scattering,* edited by H. Zabel and I. K. Robinson, Springer Proceedings in Physics Vol. 61 (Springer-Verlag, Berlin, 1992).
[17]J. Als-Nielsen, F. Christensen, and P. S. Pershan, Phys. Rev. Lett. **48**, 1107 (1982).
[18]M. K. Sanyal, S. K. Sinha, K. G. Huang, and B. M. Ocko, Phys. Rev. Lett. **66**, 628 (1991).
[19]I. M. Tidswell, T. A. Rabedeau, P. S. Pershan, and S. D. Kosowsky, Phys. Rev. Lett. **66**, 2108 (1991).
[20]M. P. Bruin, W. J. Bartels, P. Chakraborty, H. W. van Essen, J. Verhoeven, and M. J. van der Wiel, Proc. SPIE **563**, 182 (1985).
[21]J. D. Shindler and R. M. Suter, Rev. Sci. Instrum. **63**, 5343 (1992).
[22]L. G. Parratt, Phys. Rev. **95**, 1593 (1954).
[23]R. Holyst, Phys. Rev. A **44**, 3692 (1991).
[24]V. Holy, J. Kubena, I. Ohlidal, K. Lischka, and W. Plotz, Phys. Rev. B **47**, 15 896 (1993).
[25]J. B. Kortright, J. Appl. Phys. **70**, 3620 (1991).
[26]R. Schlatmann, C. Lu, J. Verhoeven, E. J. Puik, and M. J. van der Wiel, Appl. Surf. Sci. **78**, 147 (1994).
[27]J. M. Slaughter, P. A. Kearney, D. W. Schulze, C. M. Falco, C. R. Hills, E. B. Saloman, and R. N. Watts, Proc. SPIE **1343**, 73 (1990).
[28]A. Petford-Long, M. B. Stearns, C. H. Chang, D. G. Stearns, N. M. Ceglio, and A. M. Hawryluk, J. Appl. Phys. **61**, 1422 (1987).
[29]W. Lowell Morgan and D. B. Boercker, Appl. Phys. Lett. **59**, 1176 (1991).
[30]Y. H. Phang, D. E. Savage, R. Kariotis, and M. G. Lagally, J. Appl. Phys. **74**, 3181 (1993).
[31]X. M. Jiang, T.H. Metzger, and J. Peisl, Appl. Phys. Lett. **61**, 904 (1992).
[32]T. Salditt, T. H. Metzger, J. Peisl, and X. Jiang, J. Phys. III **4**, 1573 (1994).
[33]M. T. Robinson, in *Sputtering by Ion Bombardment,* edited by R. Behrisch, Springer Topics in Applied Physics Vol. 47 (Springer-Verlag, Berlin, 1981).
[34]K. H. Muller, Phys. Rev. B **35**, 7906 (1987).
[35]F. Seitz and J. S. Koehler, Solid State Phys. **2**, 305 (1956).